GROWTH AND FORMATION OF INVERSE GaP AND InP OPALS

H M Yates, D E Whitehead, M G Nolan, M E Pemble
School of Sciences, Cockcroft Building, University of Salford, Salford, M5 4WT, UK.
E Palacios-Lidon,S Rubio[1], F J Meseguer[1], C Lopez
Instituto de Ciencia de Materiales de Madrid (CSIC), Campus de Cantoblanco, E-28049, Madrid, Spain
[1]also Unidad Asociada CSIC-UPV, Av. Naranjos s/n, V-46022 Valencia, Spain.

Opals consist of an ordered array of SiO_2 spheres. This leads to a modulation of the refractive index and hence photonic stop bands behaviour over the visible/IR range of the electro-magnetic spectrum. The exact position of the stop bands depends on the size of the silica spheres. However, the refractive index contrast between the SiO_2 spheres and air spaces is not great enough to open up a full photonic band gap (PBG), only the pseudogap. To increase the contrast the air spaces are filled with a material of high refractive index such as InP or GaP. To further increase the contrast the SiO_2 is removed leaving a III-V framework as the inverse opal structure.

By use of MOCVD we have been able to infill opals with InP and GaP to such a level that has supported the inversion of the composite forming a structure of air holes within a III-V lattice. XRD and Raman confirmed the quality of the III-V infill, while the extent of the infill was studied by SEM and reflectance measurements.

INTRODUCTION

Over the last decade there has been a great interest in photonic materials, expanding from the work of Yablonovitch (1) of mechanically drilled holes in ceramic (microwave region), to extensions of Si based microelectronics (growth, lithography, etching etc) for the 'log-pile' structure in initially Si (2) and then GaAs (3). The alternative approach was to produce PBG materials by self-organisation, as seen with opal. Opal consists of a regular fcc structure of silica spheres which provides a periodic modulation of the dielectric constant. The size of the spheres controls the periodicity and the frequency of the visible/IR spectrum in which it operates. However, the dielectric contrast between the silica spheres and the air gap is low ($\varepsilon_{SiO2}/\varepsilon_{air}$ = 2/1) so leads to a pseudo-gap. The contrast can be increased by infilling the air gaps with material of a higher dielectric constant (SnO_2, GaP, InP (4,5,6)). Theoretical values (7) for a full gap need a dielectric contrast of 16. However, this requirement can be halved to a dielectric contrast of 8 if the inverted structure of a series of ordered 'air' holes is formed (8). This inversion of the composite sample would also improve the contrast yet further. As yet this has been achieved with various II-VI compounds (CdSe (9), CdS (10)), group IV (Ge (11), Si (12)) and TiO_2 (13) by use of both Silica and polymer based opals. Until recently no III-V compounds had been successfully infilled to a high enough level to allow inversion. The first success was by Golubev (14) with GaN by impregnating opals with Ga_2O_3 and heating under NH_3. In this paper we report for the first time the production of inverted III-V structures of GaP and InP. Both InP and GaP are included as the method of

production is very similar, the only difference being the reactants. Also the characterisation of the composite and inverse opal structures gives similar results.

In earlier work (6,15) we showed that InP and GaP could be placed within opal by CVD and that even low (5%) infill lead to extensive PBG changes. Further modification of the MOCVD reactor design has been carried out, such that the reactant gases are channelled over a constricted space where the opal is placed. From this it has been possible to achieve extremely high loading of the opals, such that an inverted structure has been obtained. This is presented as a major technological breakthrough, which demonstrates the feasibility of filling opaline systems with conventional III-V semiconductors, using equipment, which apart from the reactors themselves, are industry standard.

EXPERIMENTAL

The method used to produce the opals has previously been described, as has the method of sintering (16). The sintering is important as it controls the filling fraction and leads to the formation of necks between the opals, which facilitate the removal of the original opal when the inverse structure is formed. The composite III-V opal structure is soaked in a 1% HF solution for 7 hours to remove the silica. In the samples chosen the opal sphere sizes were 230nm, 310nm and 358 nm.

The composite structures are grown in a standard atmospheric MOCVD reactor (Electrogas Systems). The only modification necessary was to the actual reactor. It had previously been converted to a vertical system (5) in which the opals sat on the top of a re-designed carbon susceptor (peppered with 2 mm diameter holes) in an attempt to force the reactant gases through the opals rather than over the top surface. This, although an improvement, still left problems in that not all the opal could be over a hole in the susceptor and hence over an area where gas could flow. Also the susceptor was loose fitting, allowing another route for the reactant gases. To get round these problems a sintered quartz platform was fused to the reactor so that all the opal sits on a porous surface. However, as this does not allow efficient heating of the samples a carbon susceptor disk was made with a hole (5 mm diameter) for the sample.

Reactants used were trimethyl gallium (3.0×10^{-5} mol min^{-1}) or trimethyl indium (1.9×10^{-5} mol min^{-1}) (Epichem) with phosphine (8.9×10^{-4} mol min^{-1}) (BOC) in a carrier gas of hydrogen (1 L min^{-1}). As previously stated (17) a cyclic method is used in which the reactants are sequentially passed through the reactor to allow growth within the opal rather than on the surface. This cycle is repeated up to 10 times. Prior to growth the samples are heated to 200 ^{o}C for 1 hr to remove any moisture within the opal pores. During growth the organo-metallic is added at 50 ^{o}C and the phosphine at 400 ^{o}C at 30 minute intervals.

Characterisation was carried out with X-ray diffraction (Siemens D5000), micro-Raman 514.5 nm Ar line (Renishaw 1000) and scanning electron microscopy. To study the photonic band gap behaviour of the samples Bragg reflectance measurements were used. Incident plane parellel white light (Tungsten (NIR) and Xe arc (visible)) at 15^{o} to normal to the (111) orientation of the composite and inverse structures was used.

RESULTS AND DISCUSSION

Visually, the infilled opals are highly opalescent and deeply coloured. The actual colour seen depends on the angle it is viewed. The uniformity of the colour across the sample relates to the uniformity of the infill and quality of the opal.

The infilled GaP and InP was polycrystalline, as seen from the XRD (figure 1) with strong diffraction peaks for the (111), (220) and (311) orientations.

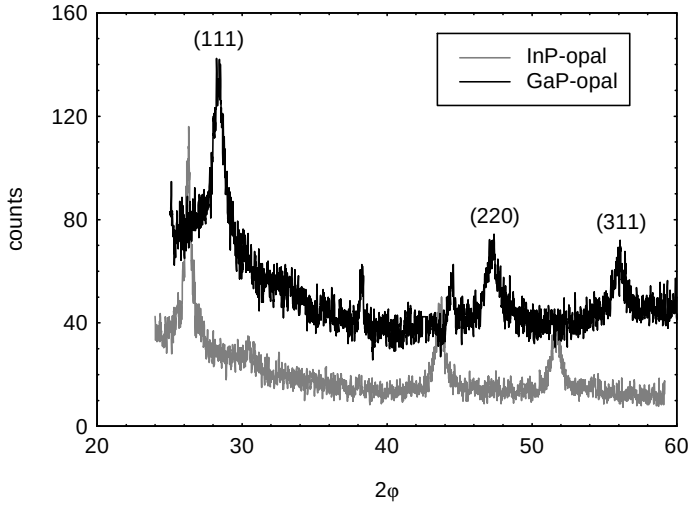

Figure 1 - X-ray diffraction of InP and GaP composite opals. The peaks at 38^{o} and 44^{o} on the GaP-opal sample come from the XRD sample holder.

Also the micro-Raman (figure 2) shows strong signals for the LO and TO phonons. However, it can be seen that the position of the GaP LO and TO phonon bands (390 cm^{-1}, 357 cm^{-1}) are at lower Raman shifts than that of bulk literature values (402, 366 cm^{-1})(18).

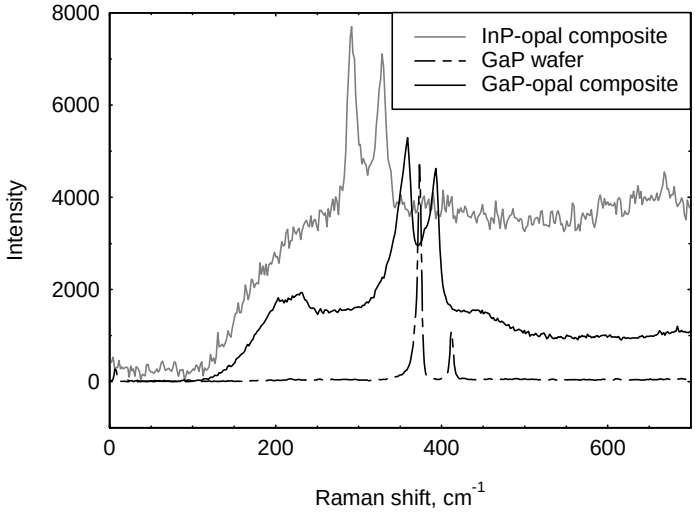

Figure 2 – Raman for the III-V composites.

This reduction in Raman shift could be due to strain within a GaP sample (19). A comparison with a GaP wafer, that should be approximately strain free, is shown to have the highest Raman shift values (411 cm^{-1}, 373 cm^{-1}). A similar result was seen for the InP with the LO and TO phonons of InP (291 cm^{-1}, 328 cm^{-1}), which again are lower than the literature values of 304 and 346 cm^{-1}. The softening of the phonons can be also due to the nanocrystalline quality of the semiconductors loaded. The Raman k-vector selection rules are relaxed in the case of amorphous and nanocrystalline semiconductors. Therefore, Raman peaks are broader and the frequency becomes softer as accurs in our case. Alternatively (or as well) it could be related to increased III-V porosity with the Raman shift to lower values (20).

SEM (Figure 3) depth profiles of a cross-section through the opal host (ϕ = 358nm) showed that it was uniformly deposited within the opal and penetrated heavily to at least 200 μm (figure 3b).

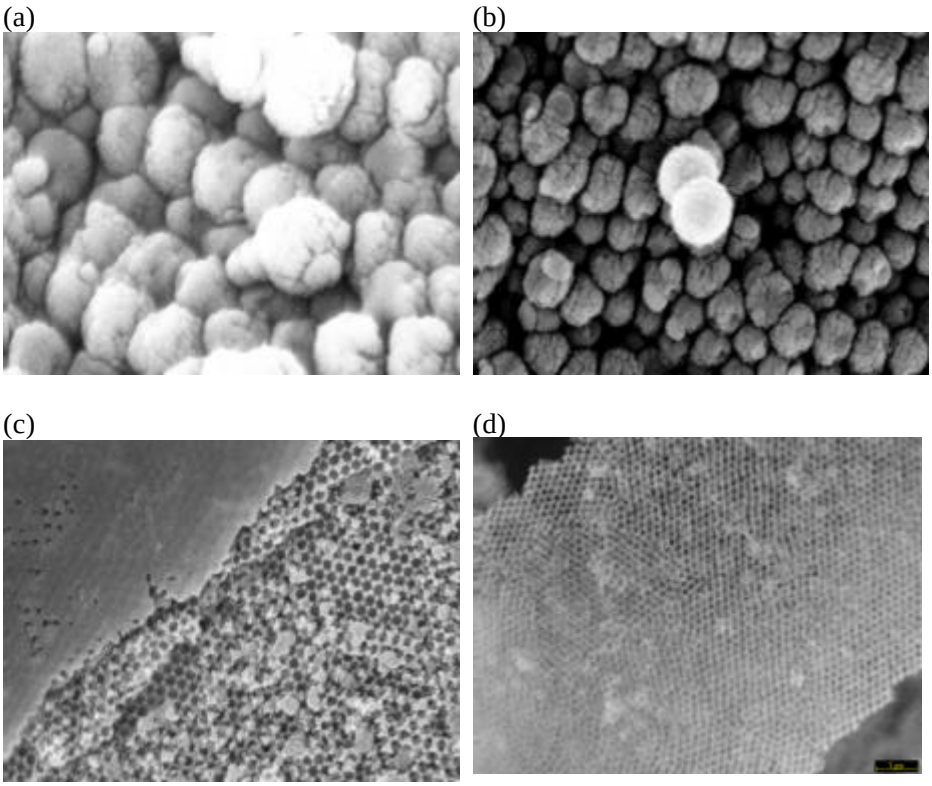

Figure 3 - SEM images (a) near surface and (b) depth of 200 μm of the interior of the GaP infilled opal sample, (c) inverted GaP opal (air holes 358 nm), (d) inverted InP opal (air holes 230 nm).

It can be seen that the GaP forms a thick skin round the opal spheres consisting of lots of small crystallites. The same type of behaviour can be seen with InP. It is possible that the infill takes place by the growth of many small independent crystallites that gradually fill up the space round the opal spheres. It was also possible to invert these structures, as seen in Figure 3c (GaP) and 3d (InP). The hexagonal structure of air holes and GaP/InP

walls can be clearly be seen. The order within the samples stretches over 10's of microns.

At a given wavelength InP and GaP have similar, but not identical, refractive indices. For example at a wavelength of 700 nm the refractive indices of InP and GaP are 3.48 and 3.23 respectively. The difference is relatively small, but it is still large enough to have an influence on the PBG effects of the infilled and inverted opals. The optical properties of the III-V opal composites and inverse structures gave broadly the same result (differences in overall intensity due to opal quality, shifts in position of the bands due to bare opal size and amount of infill). From the position of the Bragg stop band it is possible to estimate the extent of III-V infill within the opal. The higher the extent of infill the greater the wavelength shift from the bare opal.

The reflectance data is complex in the cases of InP and GaP and will be reported in more detail in another publication. In general the 1st order Bragg stop band is taken to be the most intense, well defined peak round $a/\lambda=0.65$ (see Figure 4). However, if this approach is taken, then the data (in Figure 4) implies that there is little to no shift in stop band position following infill. In fact the infill calculation predicts a level of at the most 7% pore volume. This is obviously not correct, as there is enough GaP (or InP) within the pores to support inversion. As the Bragg peak is very sensitive to the infilling it should be wider than that for the bare opal, but it is actually narrower. Finally, this peak lies to the lower wavelength side of two of the infilled samples shown, which would imply a reduction in the average refractive index of the composite opal, which is not possible.

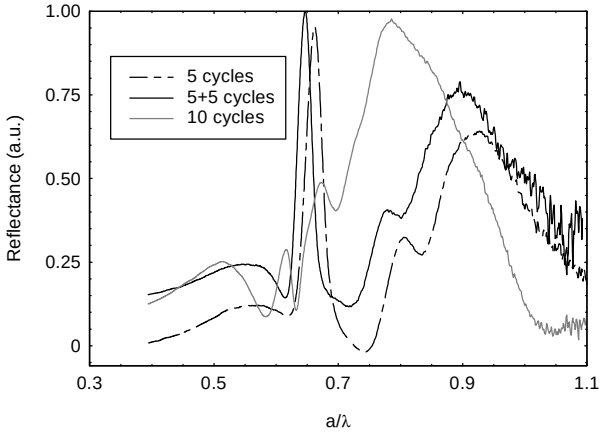

Figure 4 – Bragg diffraction showing the shift in wavelength (and hence infill for GaP) depending on the number of growth cycles. Sphere size of the bare opal used is 310 nm.

The Bragg stop band has been taken to be the higher wavelength, low intensity peak. Using this, the infill can be calculated by Bragg's Law. However, these values should only be taken as an approximate guide for comparison. Possible reasons are that Bragg's Law is only strictly accurate for weak dielectric contrast where

$(\varepsilon_1-\varepsilon_2)/(\varepsilon_1+\varepsilon_2)<1$

and that the choice of dielectric constant value in the calculation could be inaccurate due to unintentional doping (21) of the GaP or InP.

Samples were prepared in two different ways. In the first one, the sample was infilled in five growth cycles and then characterised. After this, a new infiltration (five more cycles) was carried out. The second one consisted of performing ten growth cycles, without the extraction of sample from the reactor. Reflectance measurements are shown in Figure 4 for the GaP-opal composite. For clarity the bare opal has not been shown, which consists, within this wavelength range, of a single peak at 670 nm (a/λ=0.654).

As seen in Figure 4 the Bragg peak for 10 cycles (a/λ=0.51, 52% pore volume) is at higher wavelength than that for 5+5 cycles (a/λ=0.55, 35% pore volume) which is again greater than that for 5 cycles (a/λ=0.56, 30% pore volume). From this it is obviously more efficient making the infiltration in one run of 10 cycles (peaks are shifted to higher wavelengths) than 2 runs of 5 cycles. Both these methods, as expected, infill the opal to a higher level than just 5 growth cycles. The reduced efficiency is probably due to a thin film of GaP grown on the top of the opal. This gradual closing of the opal pores reduces the amount of infiltration inside the opal. Also, the removal of the sample from the reactor leads to the influx of air and moisture, which in turn will require that the sample is re-baked before infilling. This may have a detrimental effect on the sample. Only 10 cycle growth samples support the inversion for GaP, while for InP 4 to 6 cycles (depending on the size of the opal spheres infiltrated) was sufficient. The faster growth of the InP, under the growth conditions used, may relate the difference in the Ga-C and In-C bonds in the organo-metallic reactant. The lower breaking strength (22) of the In-C bond making it more thermodynamically favourable that the trimethyl indium reacts faster, hence speeding the reaction.

Figure 5a shows the behaviour on the Bragg stop-band on changing between bare to GaP-opal composite to GaP inverse structure. As expected the bandwidth increases as the dielectric contrast increases from bare opal (silica/air 2.1 to composite 5 to inverse 10). An approximate doubling of the dielectric contrast leads to atleast a doubling of the experimental gap to mid-gap ratios $\Delta\lambda/\lambda$ (6%, 22%, 46%).

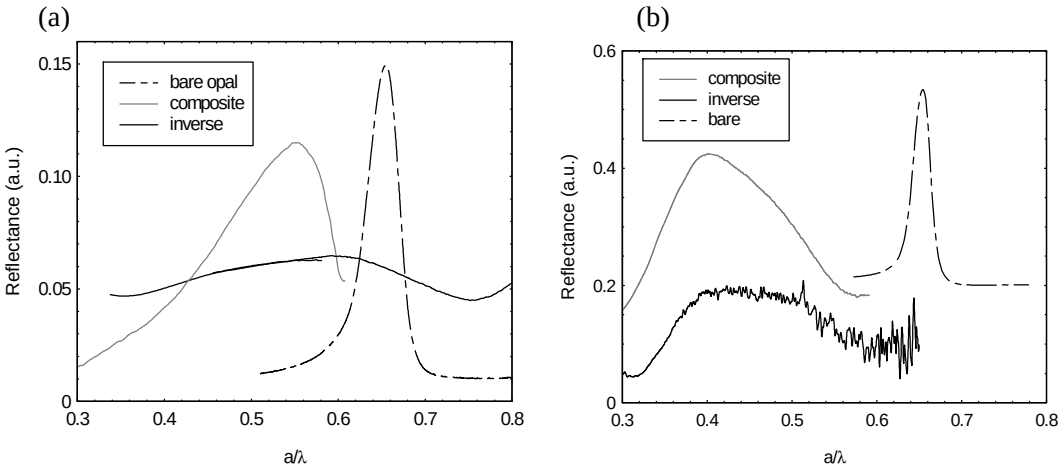

Figure 5 – Bragg reflectance of (a) GaP inverse opal, GaP-opal composite and bare opal (sphere size 358 nm) (b) InP inverse opal, InP-opal composite and bare opal (sphere size 230 nm).

This is particularly noticeable with the inverse structure as this is a much stronger scatterer due to the fill factor being 0.26 not 0.74. The position of the stop-band will basically depend on the average dielectric constant as the underlying structure is not changed on infilling or inversion. The average dielectric constant increases from that of the bare opal 1.8 to the inverse structure 2.4 (65% pore volume) (totally infilled 3.1) to the composite 3.2 (34% pore volume) (totally infilled 3.9). As this increases the stop-band energy decreases as seen in figure 5a.

This behaviour is all replicated for the equivalent InP set of structures, as seen in Figure 5b. As the opal used is much smaller (230 nm spheres rather than 358 nm) the wavelength range in which the stop bands are observed is at a lower wavelength and hence the dielectric constant used is higher. Again as the dielectric contrast increases (silica/air 2.1 to composite 6 to inverse 12.5) there is a broadening of the experimental gap to mid-gap ratios $\Delta\lambda/\lambda$ (4%, 35%, 43%). However this is greater than expected so could be due to the presence of a range of bands. The stop band energy is seen to increase from that of the composite (96% pore volume), through the inverted structure (98% pore volume), to the bare opal as the average dielectric constant decreases (4.8, 3, 1.8).

By use of a a/λ scale on the x-axis it makes it possible to compare directly the InP and GaP reflectance results, removing the differences caused by the wavelength position or opal sphere size. For both the composite and the inverse structures the shift for the GaP is less than that for the InP, which is in agreement with a lower dielectric constant average for the GaP-composite and GaP inverse structures, due to less GaP deposition. The band width of the composite is wider for InP than GaP confirming the higher dielectric constant contrast for the InP-composite. For the inverse structures the band widths are similar with greater error in their measurement.

CONCLUSIONS

Very high levels of good quality GaP and InP have been grown within the opal structures as seem by X-ray diffraction and Raman. The behaviour of the (111) Bragg peak fitted well with the expected behaviour relating to the dielectric contrast/average and the fill factor. It was found that a 10 cycle growth was necessary for inversion of the GaP structure while only 4 - 6 cycles were needed for the InP structure. These relating to the faster growth rate of InP over GaP. Also of interest was that a single experiment of 10 cycles was more efficient than 2 experiments of 5 cycles. Increased numbers of growth cycles, as expected, increased the amount of infill, but with ever decreasing amounts at each cycle due to the gradual reduction in the size of the pores within the opal. It has successfully been shown, for the first time that inverted opaline structures of GaP and InP can be grown.

ACKNOWLEGDEMENTS

This work is supported by the EC PHOBOS project 27731 and the EPSRC in the UK.

REFERENCES

1 E. Yablonovitch, T.J. Gmitter, K.M. Leung, Phys.Rev.Lett.,**67**, 2295 (1991)
2 E. Ozbay, E. Michel, G. Tuttle, R. Biswas, M. Sigalas, K.-M. Ho Appl.Phys.Lett., **64**, 2059 (1994)
3 N. Yamamoto, S. Noda, A. Chutinan, Jpn.J.Appl.Phys., **37**, L1052 (1998)
4 H.M. Yates, M.E. Pemble, A. Blanco, H. Miguez, C. Lopez, F.J. Meseguer, Chemical Vapor Deposition, **6**, 283 (2000)
5 D.E. Whitehead, M.E. Pemble, H.M. Yates, A. Blanco, C. Lopez, H. Miguez, F.J. Meseguer, J. de Physique IV,**12**, 63, (2002)
6 H. Miguez, A. Blanco F.J. Meseguer, C. Lopez, H.M. Yates, M.E. Pemble, V. Fornes, A. Mifsud, Phys.Rev.B, **59**, 1553, (1999)
7 H. Sozuer, J.Haus, R.Inguva Phys.Rev.B, **45**, 13962 (1992)
8 K. Busch, S. John, Phys.Rev.E, **58**, 3896 (1998)
9 Y.A. Vlasov, N. Yao, D.J. Norris, Adv. Mater., **11**, 165 (1999)
10 A. Blanco, H. Miguez, F. Meseguer, C. Lopez, F. Lopez-Tejeira, J. Sanchez-Dehesa, Appl.Phys.Lett., **78**, 3181 (2001)
11 H. Miguez, E. Chomski, F. Garcia-Santamaria, M. Ibisate, S. John, C. Lopez, F. Meseguer, J.P. Mondia, G.A. Ozin, O. Toader, H.M. van Driel Adv.Mater., **13**, 1634 (2001)
12 A. Blanco, E. Chomski, M. Ibisate, S. John, S.W. Leonard, C. Lopez, F. Meseguer, H. Miguez, J.P. Mondia, G.A. Ozin, O. Toader, H.M. van Driel, Nature, **405**, 437 (2000)
13 J.E.G.J. Wijnhoven, W.L.Vos, Science **281**, 802 (1998)
14 V.G. Golubev, D.A. Kurdyukov, A.V. Medvedev, A.B. Pevtsov, L.M. Sorokin, J.L. Hutchison, Semiconductors, **35**, 1320 (2001)
15 S.G. Romanov, R.M. Delarue, H.M. Yates, M.E. Pemble, J.Phys.Condens.Mat., **12**, 339 (2000)
16 H. Miguez, F. Meseguer, C. Lopez, A. Mifsud, J.S. Moya, L. Vazquez, Langmuir, **13**, 6009 (1997)
17 H.M. Yates, M.E. Pemble, H. Miguez, A. Blanco, C. Lopez, F.J. Meseguer, L. Vazquez, J.Cryst.Growth, **193**, 9, (1998)
18 D.O. Henderson, A. Veda, Y-S. Tung, R. Mu, W.C. White, R.A. Zuhr, J.G. Zhu, J.Phys.D,**30**, 1432 (1997)
19 K. Nakamura, T. Fuyuli, H. Matsunami, Jpn. J. Appl.Phys., **37**, 4231 (1998)
20 I.M. Tiginyamu, G. Irmer, J. Monecke, H.L. Hartnagel, Phys.Rev.B, **55**, 6739 (1997)
21 Y-K. Ha, J-E. Kim, H.Y. Park, C-S. Kee, H. Lim, Phys.Rev.B, **66**, 075109 (2002)
22 J.J. Coleman, Proc.IEEE, **85**, 1715 (1997)